

Electronic Structure of $\text{SrNb}_8\text{O}_{14}$ and $\text{Mg}_3\text{Nb}_6\text{O}_{11}$ Studied by Spectroscopic Methods

H. Mizoguchi,* K. Ueda,[†] K. Fukumi, N. Kitamura, Z. Siroma, T. Takeuchi, K. Kadono, H. Yanagi,[†] H. Hosono,[†] and H. Kawazoe[†]

Osaka National Research Institute, AIST, Ikeda, Osaka 563-8577, Japan

Received March 10, 2000. Revised Manuscript Received May 15, 2000

Although there are many studies about oxides containing Nb_6O_{12} cluster, the electronic structure has not been elucidated experimentally. Therefore, those around the Fermi level (E_F) for $\text{SrNb}_8\text{O}_{14}$ and $\text{Mg}_3\text{Nb}_6\text{O}_{11}$, which contain 14 valence electrons per cluster, were evaluated using electronic spectroscopies. Photoemission spectra showed that the occupied states were roughly split into two bands, and the shallower band was primarily composed of Nb 4d orbital. On the other hand, the bottom of the unoccupied state was attributed to 4d orbitals of Nb_6 cluster mainly on the basis of information obtained by inverse photoemission and Nb L₃-edge X-ray absorption near-edge structure spectra, showing that the electronic structure around E_F of these oxides were dominated by the nature of Nb_6 cluster. The optical transition in the region 0.1–4 eV was interpreted as Nb4d–4d intratomic electronic transitions, compared with those of niobium oxides. This indicates that these materials were semimetals or semiconductors with a considerable narrow band gap.

Introduction

The $\text{Nb}_6\text{O}^{12}\text{O}^{\text{a}}_6$ cluster, shown in Figure 1a, is one of the well-known metal clusters in solid oxides.¹ Twelve oxide ions (O^{i}) are coordinated on each Nb–Nb edge of Nb_6 octahedron. The six apical oxide ions (O^{a}) is located on each Nb ion. The cluster contains several Nb4d electrons, and the cluster is regarded as an electron reservoir. Therefore, it is interesting to arrange this cluster periodically in a matrix. This gives the materials great promise for optical applications such as nonlinear optical properties of semiconductor particles observed in glassy oxide matrix. However, the oxides which contain the cluster in the position apart from neighboring one do not exist scarcely. If it is realized, the lattice constants of the crystal must become very long, although such a large periodicity can be seen in the polar organic molecular-intercalated oxides such as clay.

A lot of new oxides containing the $\text{Nb}_6\text{O}^{12}\text{O}^{\text{a}}_6$ cluster have been discovered.¹ Simon et al. proved the MO diagram for $\text{Nb}_6\text{O}^{12}\text{O}^{\text{a}}_6$ cluster to be $(a_{1g})^2(t_{1u})^6(t_{2g})^6(a_{2u})^0$ in the event that 14 valence electrons occupy Nb–Nb

bonds (average Nb valence of +2.87).¹ Among such oxides, which have been known so far, it is interesting to compare the two oxides with following two linkages of the Nb_6 cluster that contains 14 valence electrons. One is $\text{SrNb}_8\text{O}_{14}$, which is represented as $(\text{SrO}) \cdot (\text{Nb}_2\text{O}_5) \cdot (\text{Nb}_6\text{O}_8)$, with the linkage toward the O^{i} direction, resulting in one-dimensional chain toward orthorhombic c axis, shown in Figure 1b.² One O^{i} and two O^{a} are shared with the cluster neighboring each other. The other is $\text{Mg}_3\text{Nb}_6\text{O}_{11}$, which is regarded as $(\text{MgO})_3 \cdot (\text{Nb}_6\text{O}_8)$, with two-dimensional linkages (Figure 1c).^{3,4} A hexagonal unit cell is applied in the c axis, perpendicular to the two-dimensional linkage.

We therefore undertook the estimation of the electronic structure of $\text{SrNb}_8\text{O}_{14}$ and $\text{Mg}_3\text{Nb}_6\text{O}_{11}$, using electronic and optical spectroscopies, and attempted to discuss it with reference to the physical properties.

Experimental Section

Polycrystalline $\text{SrNb}_8\text{O}_{14}$ was prepared from a stoichiometric mixture of SrCO_3 (99.9% pure) and Nb_2O_5 (99.9% pure). The mixture was melted by heating in a Pt crucible at 1770 K in air and quenched to room temperature. Obtained bulk material was crushed and was subsequently reduced to $\text{SrNb}_8\text{O}_{14}$ by heating at 1570 K for under Ar–60% H_2 for 50 h with several intermediate grinding. This method prevented the formation of $\text{Sr}_{0.82}\text{NbO}_3$ effectively. Polycrystalline $\text{Mg}_3\text{Nb}_6\text{O}_{11}$ was prepared from the mixture of MgCO_3 (basic) and Nb_2O_5 (99.9% pure). The mixture was heated at 1270 K for 10 h in air. Obtained MgNb_2O_6 powder was reduced to $\text{Mg}_3\text{Nb}_6\text{O}_{11}$ by heating at 1470 K under Ar–60% H_2 for 40 h, with several intermediate grinding. Each obtained powder was subsequently sintered at 1370 K for 5 min by spark plasma sintering (SPS) method with a SPS-515S (Sumitomo Coal Mining).⁵ As a reference, NbO thin film was prepared on silica glass substrate heated at 770 K, by rf magnetron reactive sputtering, using Nb plate target.

* To whom correspondence should be addressed. Present address: Hosono Transparent ElectroActive Materials, ERATO, JST, KSP C-1232, 3-2-1 Sakado, Takatsu-ku, Kawasaki 213-0012, Japan.

[†] Tokyo Institute of Technology, Materials and Structures Laboratory, Yokohama 226-8503, Japan.

(1) Kohler, J.; Svensson, G.; Simon, A. *Angew. Chem., Int. Ed. Engl.* **1992**, *31*, 1437.

(2) Kohler, J.; Simon, A.; Hibble, S. J.; Cheetham, A. K. *J. Less-Common Met.* **1988**, *142*, 123.

(3) Marinder, B. O. *Chim. Script.* **1977**, *11*, 97.

(4) Burns, R.; Kohler, J.; Simon, A. *Z. Naturforsch.* **1987**, *42b*, 536.

(5) Takeuchi, T.; Betourne, E.; Tabuchi, M.; Kageyama, H.; Kobayashi, Y.; Coats, A.; Morrison, F.; Sinclair, D. C.; West, A. R. *J. Mater. Sci.* **1999**, *34*, 917.

(6) Ueda, K.; Yanagi, H.; Hosono, H.; Kawazoe, H. *J. Phys.: Condens. Matter* **1999**, *11*, 3535.

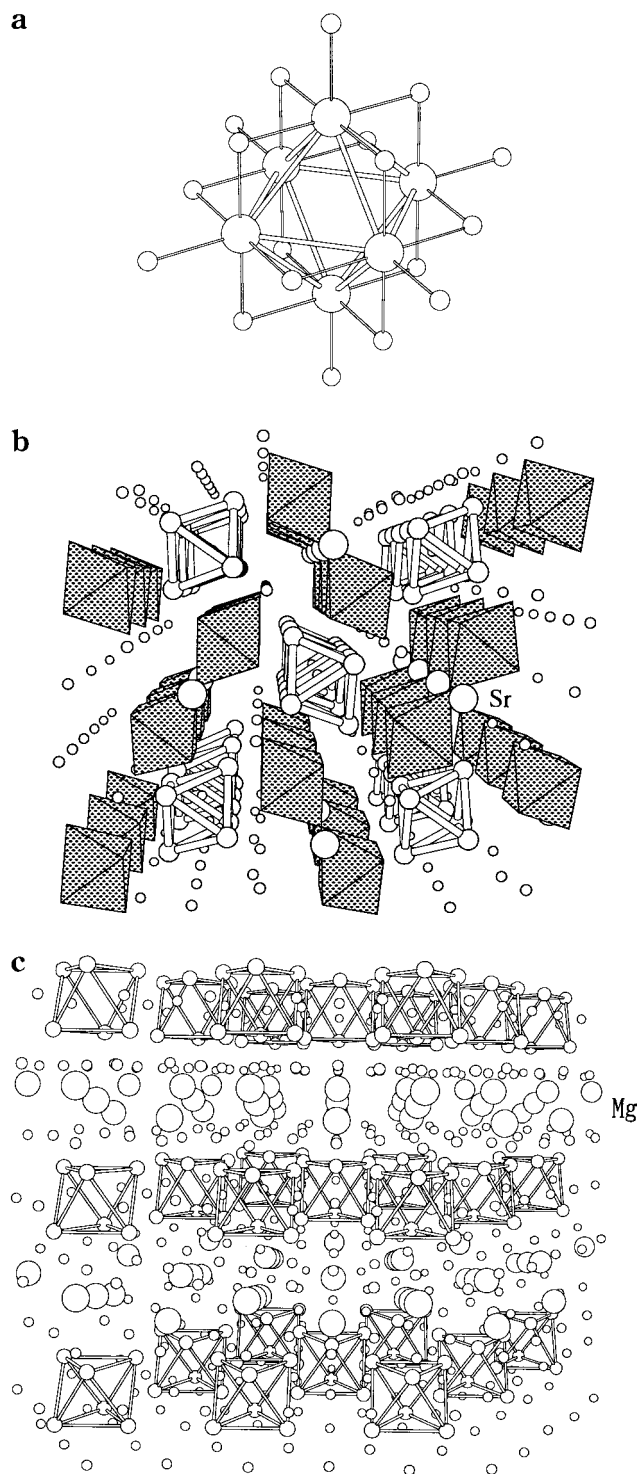


Figure 1. (a) Nb₆O₁₂O₆ clusters and structure schemes of (b) SrNb₈O₁₄ and (c) Mg₃Nb₆O₁₁. Nb⁵⁺O₆ octahedra are hatched.

The crystalline phase obtained was identified by powder X-ray diffraction (XRD) analysis (RIGAKU RAD-C, Cu K α , 40 kV, 150 mA). The composition of pellet obtained was confirmed by EDS in SEM (JEOL S-5000).

Photoemission spectra were measured using an ULVAC-Phi ESCA5300 system under 1×10^{-9} Torr to estimate occupied states. Mg K α (1253.6 eV) and HeII (40.8 eV) radiation were used as excitation sources. The total resolution of the system was about 0.5 and 0.3 eV for X-ray photoemission (XPS) spectra and ultraviolet photoemission (UPS) spectrum, respectively.

Ultraviolet inverse photoemission (UV-IPES) spectra were measured in the bremsstrahlung isochromat spectroscopy

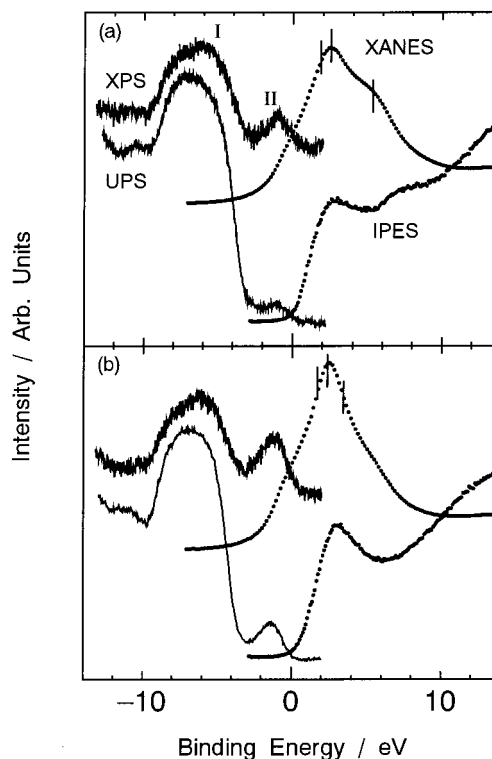


Figure 2. PES, IPES, and Nb L₃-edge XANES spectra for (a) SrNb₈O₁₁ and (b) Mg₃Nb₆O₁₁. The binding energy was measured from the E_F . The thresholds of the XANES spectra were roughly adjusted.

mode under 2×10^{-10} Torr. The luminescence of 9.5 eV was detected by electron multiplier through an SrF₂ window.^{6,7} The surface of the polycrystalline sample was scratched under 1×10^{-8} to 3×10^{-9} Torr to obtain fresh surface before the PES and IPES measurements. X-ray absorption near-edge structure (XANES) spectra of the Nb L₃-edge of the samples were measured in an electron yield mode at the BL7A of an electron storage ring (UVSOR) in the Institute for Molecular Science to examine the unoccupied states associated with the Nb ions. A Ge(111) double-crystal monochromator was used to obtain the experimental resolution of ~ 0.5 eV.

Dielectric constants and optical constants were measured by spectroscopic ellipsometry measurements at 60°, 70°, and 80° in the photon energy region 0.7–4.3 eV, using a V-VASE (J. A. Woollam). Infrared reflectivity was recorded using Perkin-Elmer 1600 IR spectrometer. DC electrical conductivity was measured by standard four-probes method in the region of 77–300 K.

Results

All the diffraction peaks of the samples in the X-ray diffraction patterns were indexed as those of SrNb₈O₁₄ (JCPDS84-1666, orthorhombic, *Pbam*, $a = 0.9252$ nm, $b = 1.029$ nm, $c = 0.5956$ nm) and Mg₃Nb₆O₁₁ (JCPDS83-2116, hexagonal, *P3m1*, $a = 0.6042$ nm, $c = 0.7467$ nm), respectively. The colors of the obtained pellets of SrNb₈O₁₄ and Mg₃Nb₆O₁₁ were dark golden brown and dark green, respectively.

Parts a and b of Figure 2 show the energy spectra (PES, IPES, and XANES) of SrNb₈O₁₄ and Mg₃Nb₆O₁₁, respectively. The PES spectra of these oxides were very similar. There were roughly two structures in the PES

(7) Mizoguchi, H.; Fukumi, K.; Kitamura, N.; Takeuchi, T.; Hayakawa, J.; Yamanaka, H.; Yanagi, H.; Hosono, H.; Kawazoe, H. *J. Appl. Phys.* **1999**, *85*, 6502.

spectra, a deeper structure (I) located around -10 to -4 eV, and a shallower structure (II) located around -3 to 0 eV. Structure II is split into two peaks in $\text{SrNb}_8\text{O}_{14}$. Structure II was enhanced in these samples under X-ray excitation. The intensity ratio (II/I) was larger in $\text{Mg}_3\text{Nb}_6\text{O}_{11}$. Clear-cuttings were not confirmed at the E_F in the oxides.

UV-IPES is one of the most powerful methods of examining unoccupied states, although the cross section of cationic d orbitals against ultraviolet light is not large. Rising point of the spectrum of these oxides was very similar. The sharp peaks around the 0 eV, which did not cross the E_F clearly were detected in $\text{SrNb}_8\text{O}_{14}$ and $\text{Mg}_3\text{Nb}_6\text{O}_{11}$. It seems that there exists another peak near 5 eV except two peaks at 2.5 and 7 eV in $\text{SrNb}_8\text{O}_{14}$. Nb $2p_{3/2} \rightarrow 4d$ electron transitions are detected in Nb L_3 edge XANES spectra. These white lines were composed of three peaks in the oxides. It is noted that the higher energy peak was located in 5.5 eV, apart from other two peaks in $\text{SrNb}_8\text{O}_{14}$.

The apparent density of the pellets was 5.60 g cm^{-3} (91% of the theoretical X-ray density) for $\text{SrNb}_8\text{O}_{14}$ or 5.10 g cm^{-3} (90% of the theoretical X-ray density) for $\text{Mg}_3\text{Nb}_6\text{O}_{11}$. The relatively high density of the pellets, which results in the lustrous appearance of their polished surface, enables us to estimate the optical properties. Optical constants estimated by spectroscopic ellipsometry are shown in Figure 3a. The sign of the real part of dielectric constant, ϵ_1 of NbO changed from plus to minus at ~ 3.2 eV. The extinction coefficient, k had a minimum value of 0.9 at 4.3 eV. The dielectric constant of $\text{SrNb}_8\text{O}_{14}$ and $\text{Mg}_3\text{Nb}_6\text{O}_{11}$ had similar spectrum shape with the maximum in ϵ_2 at 1.8 and 2.3 eV, respectively. Their signs did not change in the region $1.4 < h\nu < 4.5$ eV. Reflectivity of $\text{SrNb}_8\text{O}_{14}$ or $\text{Mg}_3\text{Nb}_6\text{O}_{11}$ in IR region was shown in Figure 3b. It goes up monotonically toward lower photon energy in the region $0.5\text{--}0.15$ eV. These oxides have many sharp and intense peaks in the region, $h\nu < 0.1$ eV. Similar intense peaks were confirmed in Nb_2O_5 in the same region.

Figure 4 shows the temperature dependence of electrical conductivity of these oxides containing Nb_6 cluster. The conductivities for $\text{SrNb}_8\text{O}_{14}$ and $\text{Mg}_3\text{Nb}_6\text{O}_{11}$ were 2 orders of magnitude smaller than that for NbO. Weak temperature dependence of the conductivities was observed in these oxides. Seebeck coefficients of these three oxides containing Nb_6 cluster were negative.

Discussion

First, occupied states of these oxides will be discussed. Occupied bands observed by PES were similar in $\text{SrNb}_8\text{O}_{14}$ and $\text{Mg}_3\text{Nb}_6\text{O}_{11}$ except for the intensity ratio of (II/I). The cross section of PES in each orbital has a large dependence on the photon energy of excitation. As it has been shown that cross section ratio, Nb4d/O2p, are 0.69 and 9.6 for HeII and Mg K α , UPS and XPS responds to both the orbitals and Nb4d, respectively.⁸ It was deduced from the cross-section ratios that structures I and II are composed mainly of Nb4d+O2p, and Nb4d, respectively. The ratio (the number of d-

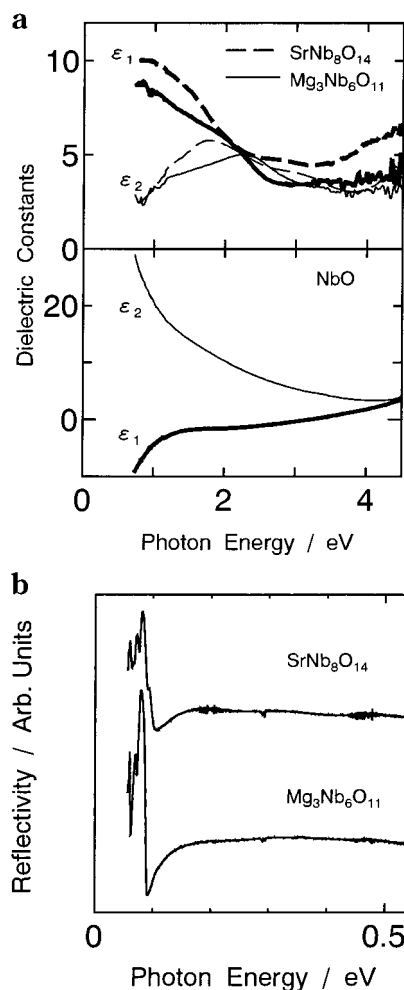


Figure 3. (a) Dielectric constants obtained by spectroscopic ellipsometry in the three oxides containing Nb_6 clusters. NbO has the defect rock-salt-type structure through introduction of vacancy, where an Nb_6 octahedron connects each other with neighboring one, sharing the six corners. (b) Reflectivity of $\text{SrNb}_8\text{O}_{14}$ and $\text{Mg}_3\text{Nb}_6\text{O}_{11}$. Al mirror was used as a reference.

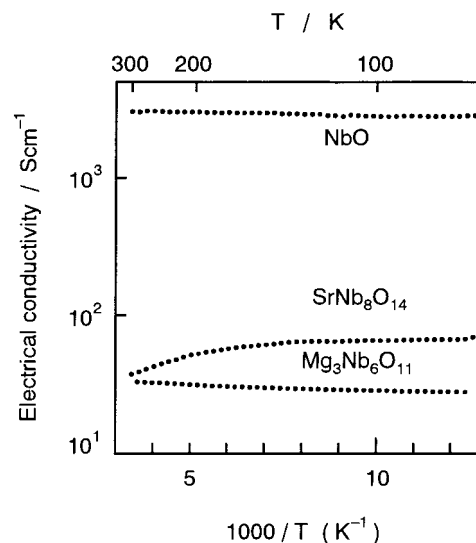


Figure 4. Electrical conductivity of $\text{SrNb}_8\text{O}_{14}$, $\text{Mg}_3\text{Nb}_6\text{O}_{11}$, and NbO, as a function of temperature.

electrons/the number of oxide ion) is 1.0 and 1.3 in $\text{SrNb}_8\text{O}_{14}$ and $\text{Mg}_3\text{Nb}_6\text{O}_{11}$, respectively. Therefore, relative intensity of II is larger in $\text{Mg}_3\text{Nb}_6\text{O}_{11}$. Careful observation shows the spectrum of structure II in these

(8) Yeh, J. J. *Atomic Calculation of Photoionization Cross-section Asymmetric Parameter*; Gordon and Breach Science Publisher: Lanthorne, PA, 1998.

compounds is composed of one or two peaks. Calculated DOS of $\text{SrNb}_8\text{O}_{14}$ by Kohler et al.¹ has three valence bands corresponding to structure II observed in PES spectra. They expected that the three peaks were due to 4d orbitals of Nb_6 cluster from their calculated partial DOS. However, the separation of three peaks was not detected clearly for structure II in PES. It is probably due to a broadening of bandwidth in polycrystalline solid, as the resolution of instruments is high enough to detect the peaks.

Second, unoccupied states of the oxide will be discussed. Now, the whole shapes of the unoccupied states for $\text{SrNb}_8\text{O}_{14}$ and $\text{Mg}_3\text{Nb}_6\text{O}_{11}$ were obtained from IPES measurements. These states are thought to be composed of Nb4d, 5s, alkali earth ion s, and d orbitals, mainly. On the other hand, XANES spectra respond to each orbital of the constitutions^{9–11} and help us to interpret the character of the unoccupied states. Normalized XANES spectra were deconvoluted to one arctan function and several Gaussian curves with a least-squares fit.¹⁰ Both spectra were best fitted with three Gaussian curves and a continuum absorption. The bars on the XANES spectra denote the peak positions of Gaussian curve estimated from deconvolution. In $\text{SrNb}_8\text{O}_{14}$, the IPES peak at 2.5 eV agreed with the two XANES peaks in the lower energy region. Therefore, the bottom of conduction band is composed of Nb4d orbitals mainly. It was difficult to consider that another IPES peak at 7 eV was attributed to unoccupied 4d states of Nb^{5+} , because it was located at too high an energy position. Therefore, we attributed the IPES peak to Sr 4d orbitals. Although the content of Sr is not large in the oxide, the DOS is thought to be considerably large, because of the narrowness of the d orbitals. Another XANES peak at 5.5 eV in $\text{SrNb}_8\text{O}_{14}$ was not observed in that of $\text{Mg}_3\text{Nb}_6\text{O}_{11}$, although both oxides contain Nb_6 cluster. Therefore, it is reasonable to consider that the peak originates from unoccupied 4d states of Nb^{5+} in $\text{SrNb}_8\text{O}_{14}$. The flat region near 5 eV was seen in IPES of $\text{SrNb}_8\text{O}_{14}$, and we considered that the region agreed with the XANES peak at 5.5 eV. Kohler et al. expected that unoccupied 4d states of Nb^{5+} was located at the position shallower than those of Nb_6 cluster on the basis of the partial DOS obtained from tight binding calculation.¹ Their result seems to support our attribution. In $\text{Mg}_3\text{Nb}_6\text{O}_{11}$, the position of the IPES peaks at 3 eV agreed well with those of all three XANES peaks. Another peak in the higher energy region was not observed in this oxide. This can be explained by the fact that Mg^{2+} ion does not have unoccupied d orbitals in the measured region. These discussions indicate that the bottom of the conduction band was therefore attributed to 4d orbitals of Nb_6 cluster, mainly.

Finally, the physical properties of these oxides containing Nb_6 cluster will be discussed on the basis of the electronic structure mentioned above. Spectroscopic ellipsometry showed that the transition from O2p to unoccupied Nb 4d orbital started at ~ 4 eV on the basis of the spectra of NbO, NbO_2 , and Nb_2O_5 , which showed

strong absorption structures in the energy region (Figure 3a). This was consistent with the PES and IPES of the oxides containing Nb_6 cluster, which showed that the transition from structure I to lowest unoccupied state started around 4 eV. Therefore, the absorption in the region $h\nu < 4$ eV was attributed to Nb4d–4d transition mainly. Spectroscopic ellipsometry in NbO which shows metallic conductivity showed that plasma frequency due to conductive carrier was 3.2 eV found by the point at $\epsilon_1 = 0$. In contrast, the sign of ϵ_1 of $\text{SrNb}_8\text{O}_{14}$ and $\text{Mg}_3\text{Nb}_6\text{O}_{11}$ did not change in the measured region 0.5–4.3 eV. The spectral change due to the transition beyond the band gap was not seen clearly in reflectivity in the IR region, even though the oscillation strength of interband transition was much smaller than that due to lattice vibration ordinary. These experimental facts suggested that $\text{SrNb}_8\text{O}_{14}$ and $\text{Mg}_3\text{Nb}_6\text{O}_{11}$ did not open the band gap, larger than 0.1 eV, indicating two possibilities: One is a semiconductive state whose band gap is narrower than 0.1 eV. In this case, the conductive carrier—electron indicated by Seebeck measurements—appears to be generated by nonstoichiometry of chemical composition. The other is a semimetallic state, having small DOS around the E_F . The electrical conductivity showed metallic or semiconductive property (Figure 4). It is reasonable to consider that the decrease of electrical conductivity relative to that of NbO originates from that of carrier concentration. Absence of plasma frequency in optical spectra can be also explained by the screening of the peaks due to lattice vibration. However, there is the possibility that the tail of plasma reflectivity appears in the range $0.3 < h\nu < 0.55$ eV. At last, we must consider an origin for the inconsistency between the conductivity and the dimension of cluster array. There are two possible reasons. One is that the contraction between clusters increases overlap of Nb4d and O2p, when we compare the distance between clusters: 0.5954 nm ($\text{SrNb}_8\text{O}_{14}$) and 0.6080 nm ($\text{Mg}_3\text{Nb}_6\text{O}_{11}$). The other is due to the difference of carrier concentration.

Conclusions

The dense polycrystalline pellets of $\text{SrNb}_8\text{O}_{14}$ and $\text{Mg}_3\text{Nb}_6\text{O}_{11}$ with a Nb_6 cluster which contains 14 valence electrons were prepared by the SPS method, and the electronic structure was investigated, using electronic spectroscopies. The results obtained are summarized below.

(1) The occupied states of these oxides were examined by PES. By taking into consideration the dependences of the ionization cross sections of each basis orbital on excitation energy, the shallowest band (II) was found to have a large Nb4d character. The other band (I) centered on -7 eV was attributed to O2p band primarily.

(2) The unoccupied states were also examined by IPES and Nb L₃-edge XANES. The coincidence of both spectra showed that the bottom of unoccupied states was composed of 4d orbital of Nb_6 cluster, mainly. Therefore, the electronic structure around E_F was dominated by that of the Nb_6 cluster.

(3) The optical constants estimated by spectroscopic ellipsometry indicated that the weak optical absorption in the region 0.1–4 eV was due to Nb4d–4d intratomic electronic transition. Deeper occupied band (I) started

(9) Sugiura, C.; Kitamura, M.; Muramatsu, S. *J. Phys. Chem. Solids* **1988**, *49*, 1095.

(10) Roth, H. F.; Meyer, G.; Hu, Z.; Kaindl, G. *Z. Anorg. Allg. Chem.* **1993**, *619*, 1369.

(11) Douillard, L.; Jollet, F.; Bellin, C.; Gautier, M.; Duraud, J. P. *J. Phys. Condens. Matter* **1994**, *6*, 5039.

to contribute to electronic transition near 4 eV. The value of electrical conductivity of these oxides was about 10^1 S cm^{-1} . However, The influence on the optical properties due to free electron was not clearly observed. These physical properties indicated that they were semi metallic or semiconductive with considerable narrow band gap.

Acknowledgment. The authors thank Dr. K. Murai in ONRI for help with ellipsometry measurements and the staff of UVSOR at the Institute for Molecular Science for help with XANES measurements. They also thank reviewers for useful suggestion.

CM0010349